

Formation of interference patterns in diffusely scattered fields with the spatial filtering of the diffraction field of a double-exposure hologram of the scatterer image focused by the Kepler telescopic system

V.G. Gusev

Tomsk State University

Received May 24, 2006

The sensitivity of a holographic interferometer to transversal or longitudinal displacements of a plane surface, diffusely scattering the light, is analyzed. It is shown that interference patterns are located in the hologram plane and in the far diffraction zone. To record these patterns, spatial filtering of the diffraction field is needed. Experimental results obtained are in a good agreement with theoretical arguments.

It was earlier shown^{1,2} that if the transversal displacement of a diffusely scattering plane surface is controlled at the double-exposure recording of a hologram of a focused image, interference patterns are located in the hologram plane and in the plane of the image of the positive lens pupil, used for the hologram recording. In this case, the sensitivity of the interferometer at recording the interference pattern, located in the hologram plane, depends both on the value and the sign of the curvature radius of the spherical wave of coherent radiation, used to illuminate the scatterer. For the interference pattern, located in the plane of the pupil image, this dependence is absent, and the interferometer sensitivity depends on the thickness of the object space in the optical scheme of the hologram recording.

The interference pattern in equal-slope fringes, characterizing the transversal displacement of the scatterer, is located in the plane of the pupil image, in which identical subjective speckles of two exposures match at the stage of hologram reconstruction, and the interferometer sensitivity depends on the thickness of the object space in the optical arrangement of the hologram recording.

In this paper, the peculiarities of formation of interference patterns, characterizing the transversal or longitudinal displacement of the diffusely scattering plane surface at the double-exposure recording of the hologram of a focused image of the scatterer with the aid of a two-component optical system are analyzed in order to determine the interferometer sensitivity. The cases that the recorded image of an object is and is not restricted by the field of view of a telecentric optical system are considered.

According to Fig. 1, the matte screen, lying in the plane (x_1, y_1) , is illuminated by the coherent radiation with the divergent spherical wave characterized by the curvature radius R . The screen image in the plane (x_3, y_3) of the photographic plate is constructed of positive lenses L_1 and L_2 with the

focal lengths f_1 and f_2 , respectively. It is assumed that the diffraction limitedness of the field is caused by the circular diaphragm p in the frequency plane (x_2, y_2) , which serves as a pupil of the two-component optical system under consideration.

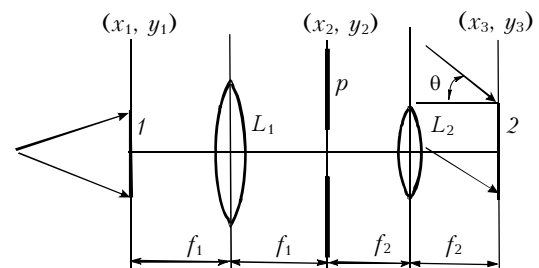


Fig. 1. Schematic of hologram recording: matte screen 1; photographic plate 2; positive lenses L_1 and L_2 ; spatial filter p in the frequency plane of the optical system.

The hologram is recorded during the first exposure with the aid of an off-axis plane reference wave. Here θ is the angle between the collimated reference beam and the normal to the plane of the photographic plate. Before the second exposure, the matte screen is displaced in its plane, for example, by the magnitude a in the direction of the axis x . Then, in the Fresnel approximation, neglecting the constant factors, the distribution of the complex amplitude of the field, corresponding to the first exposure, in the object channel in the plane (x_3, y_3) can be written in the form

$$u_1(x_3, y_3) \sim \int_{-\infty}^{\infty} \int_{-\infty}^{\infty} u_1(x_2, y_2) p(x_2, y_2) \times \exp\left[\frac{-ik(x_2x_3 + y_2y_3)}{f_2}\right] dx_2 dy_2, \quad (1)$$

where $p(x_2, y_2)$ is the pupil function³ of the two-component optical system; k is the wave number;

$$u_1(x_2, y_2) \sim \int_{-\infty}^{\infty} \int_{-\infty}^{\infty} t(x_1, y_1) \exp\left[\frac{ik}{2R}(x_1^2 + y_1^2)\right] \times \\ \times \exp\left[\frac{-ik(x_1x_2 + y_1y_2)}{f_1}\right] dx_1 dy_1; \quad (2)$$

$t(x_1, y_1)$ is the complex amplitude of transmission of the matte screen, being the random function of coordinates.

Upon the substitution of Eq. (2) into Eq. (1), we obtain

$$u_1(x_3, y_3) \sim t(-\mu x_3, -\mu y_3) \exp\left[\frac{ik\mu^2}{2R}(x_3^2 + y_3^2)\right] \otimes P(x_3, y_3), \quad (3)$$

where \otimes denotes the convolution; $\mu = f_1/f_2$ is the coefficient of the scaling transformation; $P(x_3, y_3)$ is the Fourier transform of the function $p(x_2, y_2)$ with the spatial frequencies $x_3/\lambda f_2, y_3/\lambda f_2$; λ is the wavelength of the coherent light source, used at the stages of hologram recording and reconstruction.

It follows from Eq. (3) that every point of the object image in the plane (x_3, y_3) is widened to the size of a subjective speckle, determined by the width of the function $P(x_3, y_3)$, which is the result of diffraction of the plane wave at the diaphragm p (see Fig. 1).

The distribution of the complex amplitude of the field, corresponding to the second exposure, in the object channel in the plane (x_3, y_3) is determined by the below equation, as $t(x_1, y_1)$ in Eq. (2) is replaced with $t(x_1 + a, y_1)$,

$$u_2(x_3, y_3) \sim t(-\mu x_3 + a, -\mu y_3) \times \\ \times \exp\left[\frac{ik\mu^2}{2R}(x_3^2 + y_3^2)\right] \otimes P(x_3, y_3). \quad (4)$$

Based on Refs. 4 and 5:

$$u_2(x_2, y_2) \sim \exp(ika x_2/f_1) F(x_2, y_2) \otimes \\ \otimes \exp\left[-\frac{ikR}{2f_1^2}(x_2^2 + y_2^2)\right] = \exp(ika x_2/f_1) \times \\ \times \left\{ F(x_2, y_2) \otimes \exp(-ika x_2/f_1) \exp\left[-\frac{ikR}{2f_1^2}(x_2^2 + y_2^2)\right] \right\}, \quad (5)$$

where $F(x_2, y_2)$ is the Fourier transform of $t(x_1, y_1)$ with the spatial frequencies $x_2/\lambda f_1, y_2/\lambda f_1$.

After substitution of the right-hand side of Eq. (5) into Eq. (1), in place of $u_1(x_2, y_2)$ we obtain

$$u_2(x_3, y_3) \sim t(-\mu x_3, -\mu y_3) \times \\ \times \exp\left\{\frac{ik\mu^2}{2R}[(x_3 + a/\mu)^2 + y_3^2]\right\} \otimes P(x_3 - a/\mu, y_3). \quad (6)$$

According to Eqs. (3) and (6), if the double-exposure hologram is recorded on the linear part of

the photomaterial blackening curve, the distribution of the complex amplitude of the hologram transmission, corresponding to the (-1) -st diffraction order, takes the form

$$\tau(x_3, y_3) \sim \exp(-ikx_3 \sin\theta) \times \\ \times \left\{ t(-\mu x_3, -\mu y_3) \exp\left[\frac{ik\mu^2}{2R}(x_3^2 + y_3^2)\right] \otimes P(x_3, y_3) + \right. \\ \left. + t(-\mu x_3, -\mu y_3) \exp\left\{\frac{ik\mu^2}{2R}[(x_3 + a/\mu)^2 + y_3^2]\right\} \otimes \right. \\ \left. \otimes P(x_3 - a/\mu, y_3) \right\}. \quad (7)$$

According to Eq. (7), subjective speckles, corresponding to the second exposure, are shifted in the hologram plane in the direction, opposite to the direction of the scatterer displacement, by the distance, dependent on the magnification of the optical system and independent of the curvature radius R . In addition, they are sloped at angle $a\mu/R$ with identical speckles, corresponding to the first exposure. The angle depends on the curvature radius of the spherical wave of the radiation, used to illuminate the scatterer, and the slope angle changes the sign to the opposite one, if the matte screen 1 (see Fig. 1) is illuminated by the radiation with the convergent spherical wave. In its turn, the uniform shift of speckles in the hologram plane causes, as in Refs. 1 and 2, the formation of interference patterns in the plane, in which the identical spectra of the both exposures coincide, while the slope of speckles causes the location of the interference pattern in the hologram plane.

At the stage of hologram reconstruction, the spatial filtering of the diffraction field is performed in the hologram plane with the aid of a round hole in the opaque screen p_0 (Fig. 2).

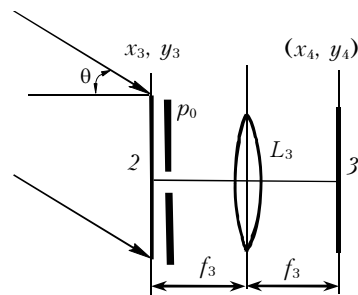


Fig. 2. Schematic of recording of the interference pattern located in the Fourier plane: hologram 2; recording plane 3; positive lens L_3 ; spatial filter p_0 .

We assume that within the diameter of the filtering aperture the change in the phase $k\mu a x_3/R$ does not exceed π and, in the general case, the center of the filtering aperture has coordinates $x_{03}, 0$. Then the distribution of the complex amplitude of the field at the output of the spatial filter is described by the equation

$$\begin{aligned}
 u(x_3, y_3) \sim & p_0(x_3, y_3) \left\{ t(-\mu x_3 - \mu x_{03}, -\mu y_3) \times \right. \\
 & \times \exp\left\{ \frac{ik\mu^2}{2R} [(x_3 + x_{03})^2 + y_3^2] \right\} \otimes P(x_3, y_3) + \\
 & + \exp\left(\frac{ika^2}{2R} \right) \exp(ik\mu a x_{03}/R) t(-\mu x_3 - \mu x_{03}, -\mu y_3) \times \\
 & \times \exp\left\{ \frac{ik\mu^2}{2R} [(x_3 + x_{03})^2 + y_3^2] \right\} \otimes \\
 & \left. \otimes \exp(-ik\mu a x_3/R) P(x_3 - a/\mu, y_3) \right\}, \quad (8)
 \end{aligned}$$

based on which the distribution of the complex amplitude of the field in the back focal plane (x_4, y_4) of L_3 with the focal length $f_3 = f_2$ (for brevity) takes the form

$$\begin{aligned}
 u(x_4, y_4) \sim & \left\{ \exp(-ik\mu x_{03} x_4/f_2) F(x_4, y_4) \otimes \right. \\
 & \otimes \exp(ikx_{03} x_4/f_2) \exp\left[-\frac{ikR}{2f_1^2} (x_4^2 + y_4^2) \right] \times \\
 & \times \left\{ p(x_4, y_4) + p\left(x_4 + \frac{f_1}{R} a, y_4 \right) \times \right. \\
 & \left. \left. \times \exp\left[i\left(-\frac{ka^2}{2R} + \frac{k\mu a x_{03}}{R} - \frac{kax_4}{f_1} \right) \right] \right\} \right\} \otimes P_0(x_4, y_4), \quad (9)
 \end{aligned}$$

where $F(x_4, y_4)$, $P_0(x_4, y_4)$ are, respectively, the Fourier transforms of the functions $t(-\mu x_3, -\mu y_3)$, $p_0(x_3, y_3)$ with spatial frequencies $x_4/\lambda f_2$, $y_4/\lambda f_2$; $p_0(x_3, y_3)$ is the transmission function of the spatial filter.

If in Eq. (9) the period of variation of $1 + \exp(ika x_4/f_1)$ exceeds at least by an order of magnitude⁷ the width of $P_0(x_4, y_4)$, determining the size of the subjective speckle in the recording plane 3 (see Fig. 2), then the illumination distribution in the recording plane within the overlap of two images of the two-component optical system pupil is determined by the equation

$$\begin{aligned}
 I(x_4, y_4) \sim & \left\{ 1 + \cos\left(-\frac{ka^2}{2R} + \frac{k\mu a x_{03}}{R} - \frac{kax_4}{f_1} \right) \right\} \times \\
 & \times \left| p(x_4, y_4) \left\{ \exp\left(\frac{-ik\mu x_{03} x_4}{f_2} \right) F(x_4, y_4) \otimes \right. \right. \\
 & \left. \left. \otimes \exp\left(\frac{ikx_{03} x_4}{f_2} \right) \exp\left[-\frac{ikR}{2f_1^2} (x_4^2 + y_4^2) \right] \right\} \otimes P_0(x_4, y_4) \right|^2. \quad (10)
 \end{aligned}$$

It follows from Eq. (10) that, taking into account that af_1/R is small within the image of the pupil of the two-component optical system, the subjective speckle structure is modulated by interference fringes, alternating on the axis x with the period $\Delta x_4 = \lambda f_1/a$, independent of the curvature radius R . As the center of the filtering aperture shifts, the behavior of the interference fringes is the following: due to the term $k\mu a x_{03}/R$ in Eq. (10), the phase of the interference pattern changes by π , when the center of the filtering aperture displaces, for example, from the minimum of an interference fringe for the interference pattern located in the hologram plane to its maximum.

If at the stage of hologram reconstruction the spatial filtering of the diffraction field is performed in the Fourier plane (x_4, y_4) (Fig. 3) and within the diameter of the filtering aperture the change in the phase kax_4/f_1 does not exceed π , then, provided that the field is not diffraction-limited due to the finite size of the aperture of the lens L_3 , the distribution of the complex amplitude of the field at the output of the filtering aperture, whose center has the coordinates $x_{04}, 0$, takes the form

$$\begin{aligned}
 u(x_4, y_4) \sim & p_0(x_4, y_4) \left\{ F(x_4 + x_{04}, y_4) \otimes \right. \\
 & \otimes \exp\left\{ -\frac{ikR}{2f_1^2} [(x_4 + x_{04})^2 + y_4^2] \right\} + \\
 & + F(x_4 + x_{04}, y_4) \otimes \exp(ika x_4/f_1) \times \\
 & \left. \times \exp\left\{ -\frac{ikR}{2f_1^2} [(x_4 + x_{04})^2 + y_4^2] \right\} \right\}, \quad (11)
 \end{aligned}$$

where $p_0(x_4, y_4)$ is the transmission function of the spatial filter.

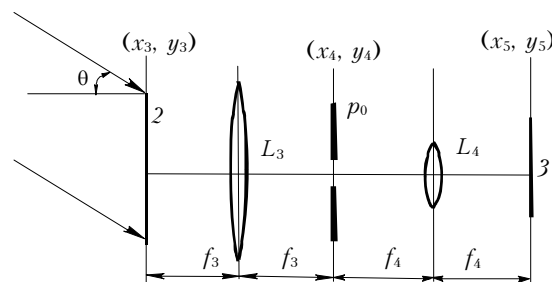


Fig. 3. Schematic of recording of the interference pattern, located in the hologram plane: hologram 2; recording plane 3; positive lenses L_3, L_4 ; spatial filter p_0 .

Assume, for brevity, that the focal length f_4 of L_4 (see Fig. 3) is equal to f_2 . Then, once the Fourier transform is performed on the basis of the distribution of the complex amplitude of the field in the plane (x_5, y_5) , obtained in this way, the illumination distribution in this plane is described by the equation

$$I(x_5, y_5) \sim \left\{ 1 + \cos \left[\frac{ka^2}{2R} - \frac{k}{f_1} x_{04} x_5 - \frac{k\mu}{R} a x_5 \right] \right\} \times \\ \times \left| t(\mu x_5, \mu y_5) \exp \left[\frac{ik\mu^2}{2R} (x_5^2 + y_5^2) \right] \right| \times \\ \times \exp(i2kx_{04} x_5 / f_2) \otimes P_0(x_5, y_5) \quad (12)$$

where $P_0(x_5, y_5)$ is the Fourier transform of the function $p_0(x_4, y_4)$ with the spatial frequencies $x_5/\lambda f_2$, $y_5/\lambda f_2$.

According to Eq. (12), in the recording plane \mathcal{B} (see Fig. 3) the interference pattern in the form of interference fringes, intermittent periodically on the axis x , modulates the subjective speckle structure within the scatterer image. The period $\Delta x_5 = \lambda |R|/\mu a$ of interference fringes depends on the magnification of the two-component optical system and the curvature radius of the spherical wave of the coherent radiation, used to illuminate the scatterer. In addition, as the center of the filtering aperture shifts, the behavior of the interference fringes is the following: due to the term $kx_{04} x_5 / f_1$ in Eq. (12) the phase of the interference pattern changes by π , as the center of the filtering aperture moves, for example, from the minimum of the interference fringe for the interference pattern located in the Fourier plane to its maximum.

The above analysis of the formation of interference patterns, characterizing the transversal displacement of the diffusely scattering plane surface shows that, in contrast to Refs. 1 and 2, the sensitivity of the interferometer in the case of recording of the interference pattern located in the hologram plane does not depend on the sign of the curvature radius R of the spherical wave for the radiation, used to illuminate the scatterer. The illumination of the scatterer by the collimated beam is accompanied, at the stage of hologram reconstruction, by the formation of "frozen" interference fringes in the Fourier plane. The recording of these fringes does not require the spatial filtering of the diffraction field in the hologram plane. In addition, the phenomenon of parallax of interference fringes is characteristic under the above recording conditions, as follows from the form of Eqs. (10) and (12).

Assume that, before the second exposure of the photographic plate, the matte screen 1 (see Fig. 1) is shifted along the z axis by $\Delta l = f'_1 - f_1$. Then, in the approximation used for $\Delta l \ll f_1$, the distribution of the complex field amplitude, corresponding to the second exposure, in the plane (x_2, y_2) takes the form

$$u'_2(x_2, y_2) \sim \exp(ik\Delta l) \exp \left[-\frac{ik\Delta l}{2f_1^2} (x_2^2 + y_2^2) \right] \times \\ \times \left\{ F(x_2, y_2) \otimes \exp \left[-\frac{ik(R - \Delta l)}{2f_1^2} (x_2^2 + y_2^2) \right] \right\}. \quad (13)$$

Consequently, the substitution of Eq. (13) in Eq. (1) for $u_1(x_2, y_2)$ yields

$$u'_2(x_3, y_3) \sim \exp(ik\Delta l) t(-\mu x_3, -\mu y_3) \times \\ \times \exp \left[\frac{ik\mu^2}{2(R - \Delta l)} (x_3^2 + y_3^2) \right] \otimes \\ \otimes \exp \left[\frac{ik\mu^2}{2\Delta l} (x_3^2 + y_3^2) \right] \otimes P(x_3, y_3). \quad (14)$$

Based on Eqs. (3) and (14), the distribution of the complex amplitude of transmittance of the double exposure hologram, corresponding to the (-1) st diffraction order for $\Delta l \ll R$, is determined by the following equation:

$$\tau'(x_3, y_3) \sim \exp(-ikx_3 \sin \theta) \left\{ t(-\mu x_3, -\mu y_3) \times \right. \\ \times \exp \left[\frac{ik\mu^2}{2R} (x_3^2 + y_3^2) \right] \otimes P(x_3, y_3) + \exp(ik\Delta l) \times \\ \times t(-\mu x_3, -\mu y_3) \exp \left[\frac{ik\mu^2}{2R} (x_3^2 + y_3^2) \right] \exp \left[\frac{ik\mu^2 \Delta l}{2R^2} (x_3^2 + y_3^2) \right] \otimes \\ \left. \otimes \exp \left[\frac{ik\mu^2}{2\Delta l} (x_3^2 + y_3^2) \right] \otimes P(x_3, y_3) \right\}. \quad (15)$$

According to Eq. (15), the subjective speckles of the both exposures coincide in the hologram plane. In this case, the speckles, corresponding to the second exposure, are broadened up to

$$P(x_3, y_3) \otimes \exp \left[\frac{ik\mu^2}{2\Delta l} (x_3^2 + y_3^2) \right].$$

In addition, the slope of speckles corresponding to the second exposure changes along the radius from the optical axis, and the sign of the slope, depending on μ and R , changes to the opposite one, as the matte screen 1 (see Fig. 1) is illuminated by radiation with the convergent spherical wave. In its turn, as in the case of control over the transversal displacement of the scatterer, interference patterns characterizing the longitudinal displacement of the diffusely scattering plane surface should be located in two planes: in the hologram plane and in the plane, in which identical speckles of the both exposures are matched.

If at the stage of hologram reconstruction (see Fig. 2) the spatial filtering of the diffraction field is performed and the change of the phase $k\mu^2 \Delta l x_3^2 / 2R^2$ within the filtering aperture at the coordinates x_{03} , 0 does not exceed π , then the distribution of the complex amplitude of the field at the output of the spatial filter takes the form

$$\begin{aligned}
u'(x_3, y_3) \sim & p_0(x_3, y_3) \left\{ t(-\mu x_3 - \mu x_{03}, -\mu y_3) \times \right. \\
& \times \exp\left\{ \frac{i k \mu^2}{2R} [(x_3 + x_{03})^2 + y_3^2] \right\} \otimes \\
& \otimes P(x_3, y_3) + \exp(i k \Delta l) \exp\left(\frac{i k \mu^2 \Delta l}{2R^2} x_{03}^2 \right) \times \\
& \times t(-\mu x_3 - \mu x_{03}, -\mu y_3) \exp\left\{ \frac{i k \mu^2}{2R} [(x_3 + x_{03})^2 + y_3^2] \right\} \otimes \\
& \left. \otimes \exp\left[\frac{i k \mu^2}{2\Delta l} (x_3^2 + y_3^2) \right] \otimes P(x_3, y_3) \right\}. \quad (16)
\end{aligned}$$

Based on this equation, after the Fourier transform, we obtain the distribution of the complex amplitude of the field in the back focal plane (x_4, y_4) of the lens L_3 (see Fig. 2) with the focal length $f_3 = f_2$, that is,

$$\begin{aligned}
u'(x_4, y_4) \sim & p(x_4, y_4) \left\{ \left[1 + \exp(i k \Delta l) \exp\left(\frac{i k \mu^2 \Delta l}{2R^2} x_{03}^2 \right) \right] \times \right. \\
& \times \exp\left[-\frac{i k \Delta l (x_4^2 + y_4^2)}{2f_1^2} \right] \left\{ \exp(-i k \mu x_{03} x_4 / f_2) F(x_4, y_4) \otimes \right. \\
& \left. \left. \otimes \exp\left[-\frac{i k R}{2f_1^2} (x_4^2 + y_4^2) \right] \exp(i k x_{03} x_4 / f_2) \right\} \otimes P_0(x_4, y_4) \right\}. \quad (17)
\end{aligned}$$

If in Eq. (17) the period of variation of $1 + \exp[-i k \Delta l (x_4^2 + y_4^2) / (2f_1^2)]$ exceeds the width of $P_0(x_4, y_4)$, by at least an order of magnitude, then the illumination distribution in the recording plane 3 (see Fig. 2) is determined by the expression

$$\begin{aligned}
I'(x_4, y_4) \sim & \left\{ 1 + \cos\left[k \Delta l + \frac{k \mu^2 \Delta l}{2R^2} x_{03}^2 - \frac{k \Delta l (x_4^2 + y_4^2)}{2f_1^2} \right] \right\} \times \\
& \times \left| p(x_4, y_4) \left\{ \exp\left(-\frac{i k \mu x_{03} x_4}{f_2} \right) F(x_4, y_4) \otimes \right. \right. \\
& \left. \left. \otimes \exp(i k x_{03} x_4 / f_2) \exp\left[-\frac{i k R}{2f_1^2} (x_4^2 + y_4^2) \right] \right\} \otimes P_0(x_4, y_4) \right|^2. \quad (18)
\end{aligned}$$

It follows from Eq. (18) that, within the pupil image of the two-component optical system (see Fig. 1), the subjective speckle structure is modulated by fringes of equal slope, i.e., by the system of concentric rings. The ring radii are independent of the curvature radius R . In addition, as the center of the filtering aperture shifts, the behavior of interference fringes consists in the following: due to the term $k \mu^2 \Delta l x_{03}^2 / 2R^2$ in Eq. (18), the phase of the interference pattern changes by π , as the center of the filtering aperture moves, for example, from the minimum to the maximum of an interference fringe

for the interference pattern located in the hologram plane.

If at the stage of hologram reconstruction the spatial filtering of the diffraction field is performed in the Fourier plane (x_4, y_4) (see Fig. 3) and the phase change $k \Delta l x_4^2 / 2f_1^2$ does not exceed π within the filtering aperture centered at the coordinates $x_{04}, 0$, then the distribution of the complex amplitude of the field at the output of the spatial filter with regard for the aforesaid takes the form

$$\begin{aligned}
u'(x_4, y_4) \sim & p_0(x_4, y_4) \left\{ F(x_4 + x_{04}, y_4) \otimes \right. \\
& \otimes \exp\left\{ -\frac{i k R}{2f_1^2} [(x_4 + x_{04})^2 + y_4^2] \right\} + \exp(i k \Delta l) \times \\
& \times \exp\left(-\frac{i k \Delta l x_{04}^2}{2f_1^2} \right) \left\{ F(x_4 + x_{04}, y_4) \otimes \right. \\
& \left. \left. \otimes \exp\left\{ -\frac{i k (R - \Delta l)}{2f_1^2} [(x_4 + x_{04})^2 + y_4^2] \right\} \right\} \right\}. \quad (19)
\end{aligned}$$

Then after the Fourier transform based on the thus obtained distribution of the complex amplitude of the field in the plane (x_5, y_5) (see Fig. 3), the illumination distribution in this plane is determined by the expression

$$\begin{aligned}
I'(x_5, y_5) \sim & \left\{ 1 + \cos\left[k \Delta l - \frac{k \Delta l x_{04}^2}{2f_1^2} + \frac{k \mu^2 \Delta l (x_5^2 + y_5^2)}{2R^2} \right] \right\} \times \\
& \times \left| t(\mu x_5, \mu y_5) \exp\left[\frac{i k \mu^2}{2R} (x_5^2 + y_5^2) \right] \exp(i 2 k x_{04} x_5 / f_2) \otimes \right. \\
& \left. \otimes P_0(x_5, y_5) \right|^2. \quad (20)
\end{aligned}$$

According to Eq. (20), the interference pattern in the recording plane 3 (see Fig. 3) formed by fringes of equal slope modulates the subjective speckle structure within the scatterer image. The radii of interference fringes depend on μ and R . In addition, as the center of the filtering aperture displaces, the behavior of interference fringes is the following: due to the term $k \Delta l x_{04}^2 / 2f_1^2$ in Eq. (20), the phase of the interference pattern changes by π , as the center of the filtering aperture moves, for example, from the minimum of an interference fringe to the maximum for the interference pattern located in the Fourier plane.

The above analysis of formation of interference patterns characterizing the longitudinal displacement of the diffusely scattering plane surface shows that, in contrast to Refs. 1 and 2, the interference pattern is located both in the plane of formation of the pupil image of the two-component optical system used for the hologram recording and in the hologram plane.

In the one-component optical system, which constructs the real image of the scatterer illuminated by coherent radiation with the spherical wave, speckles corresponding to the second exposure shift

inhomogeneously with respect to the identical speckles of the first exposure in the Fourier plane along the radius from the optical axis. On the one hand, this leads to decorrelation of waves of the both exposures, diffracting on the hologram. On the other hand, the following Fresnel transformation, performed to obtain the distribution of the complex amplitude of the field in the hologram plane, leads to the inhomogeneous action of defocusing in the hologram plane on each individual speckle. Taking into account the properties of subjective speckles, the last circumstance is accompanied by the specific intensity redistribution in the plane of formation of the pupil image of the positive lens,^{1,2} when the spatial filtering of the diffraction field is performed at the stage of reconstruction of the double-exposure hologram. The action of defocusing on individual speckles is inhomogeneous also in the case that the scatterer is illuminated by a collimated beam, when the waves of the both exposures, diffracting at the hologram, appear to be fully correlated (within the entire image space of the scatterer), since the Fourier transforms of the complex object transmission amplitude are identical for the two exposures in the Fourier plane.

In the two-component optical system considered (see Fig. 1), the distribution of the complex amplitude of the field in the plane of formation of the scatterer image results from two lens Fourier transforms. That is why decorrelation of the waves of two exposures, diffracting at the hologram, is absent and defocusing exerts the identical action on each individual subjective speckle in the plane of formation of the scatterer image. Owing to these two circumstances, interference patterns characterizing the longitudinal displacement of the diffusely scattering plane surface can be located in two planes. If an interference pattern located in the hologram plane is recorded, the interferometer sensitivity depends on the curvature radius of the spherical wave used to illuminate the scatterer. The illumination of the scatterer by the collimated beam is accompanied by the formation of "frozen" interference fringes in the Fourier plane at the stage of hologram reconstruction. The recording of these fringes does not require the spatial filtering of the diffraction field in the hologram plane. An additional characteristic feature is the absence of parallax of interference fringes under the recording conditions stated above, as follows from the form of Eqs. (18) and (20).

In the experiment, the double-exposure holograms of the focused image of the matte screen were recorded on a Mikrat-VRL photographic plates using radiation of a He-Ne laser at a wavelength of $0.63 \mu\text{m}$. The image was constructed with the aid of the positive lens L_1 with a focal length $f_1 = 250 \text{ mm}$ and a diameter of 55 mm and the positive lens L_2 with a focal length $f_2 = 220 \text{ mm}$ and a diameter of 50 mm . The diameter of the diaphragm p (see Fig. 1) was equal to 25 mm , whereas the diameter of the illuminated area of the matte screen was 35 mm . The reference beam made an angle of 10° with the normal

to the plane of the photographic plate. The experimental technique consisted in the comparison of holograms recorded both for fixed values of the transversal displacement of the scatterer $a = (0.03 \pm 0.002) \text{ mm}$ and for the longitudinal displacement $\Delta l = (2 \pm 0.002) \text{ mm}$, and the curvature radius of the spherical wave of radiation used to illuminate the matte screen ranged within $200 \leq |R| \leq \infty$.

As an example, Figure 4 shows interference patterns located in the hologram plane and characterizing the transversal displacement of the scatterer. The matte screen is marked by letter T .

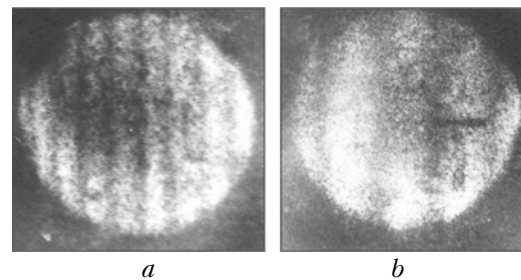


Fig. 4. Interference patterns: the screen is illuminated by radiation with divergent (*a*) and convergent (*b*) spherical waves.

The interference patterns were recorded with the spatial filtering of the diffraction field in the back focal plane of the positive lens L_3 (see Fig. 3) with a focal length of 300 mm and a diameter of 90 mm and with a filtering aperture diameter of 2 mm . Figure 4*a* corresponds to the case that the scatterer at the stage of recording of a double-exposure hologram is illuminated by radiation with the divergent spherical wave with $R = 200 \text{ mm}$, whereas Figure 4*b* corresponds to the convergent spherical wave with $R = 400 \text{ mm}$. In these two cases, as well as in the following ones connected with the change in the value and the sign of the curvature radius, the periods of interference fringes were measured and corresponded to $\Delta x_3 = \lambda|R|/\mu a$ accurate to the experimental error (10%). In addition, in all cases of the double-exposure recording of the hologram in order to determine the transversal displacement of the scatterer, the interference pattern (Fig. 5*a*) located in the plane of the pupil image of the two-component optical system (see Fig. 1) had the same frequency of interference fringes $\Delta x_4 = \lambda f_1/a$.

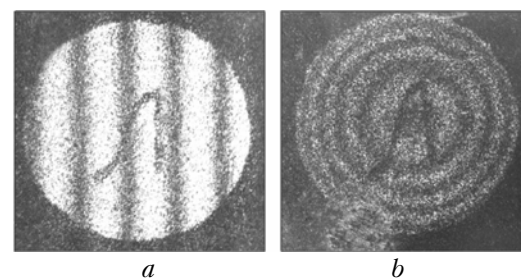


Fig. 5. Interference patterns located in the Fourier plane and characterizing: (*a*) transversal and (*b*) longitudinal displacement of the scatterer.

The thin glass plate lying in the plane (x_2, y_2) (see Fig. 1) was marked with the letter L. The interference pattern (see Fig. 5a) was recorded as shown in Fig. 2 with the spatial filtering of the diffraction field in the hologram plane through its reconstruction by a small-aperture (≈ 2 mm) laser beam. In the case that the scatterer at the stage of hologram reconstruction was illuminated by the collimated beam, the spatial filtering of the diffraction field was not necessary for the recording of the interference pattern located in the Fourier plane.

The interference patterns in Fig. 6 are located in the hologram plane and characterize the longitudinal displacement of the diffusely scattering plane surface. They were recorded similarly to the recording of interference patterns characterizing the transversal displacement of the scatterer and located in the hologram plane. Figure 6a corresponds to the case that matte screen 1 (see Fig. 1) is illuminated by the radiation with the divergent spherical wave characterized by a curvature radius $R = 250$ mm, whereas Figure 6b corresponds to the case of the convergent spherical wave with $R = 360$ mm. In these two cases, as well as in the following ones connected with the change in the value and the sign of the curvature radius, the radii of interference fringes in neighboring interference orders were measured and then used to determine the longitudinal displacement of the scatterer for the known values of λ , μ , and $|R|$ in Eq. (20). The determined displacement corresponded to $\Delta l = 2$ mm given above accurate to the experimental error (10%).

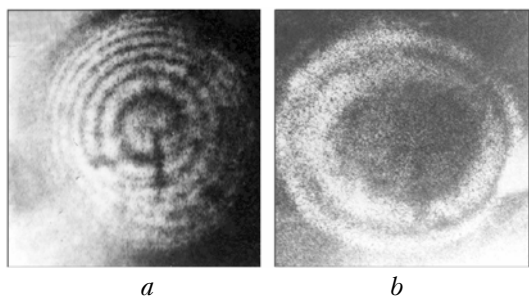


Fig. 6. Interference patterns: the matte screen is illuminated by radiation with divergent (a) and convergent (b) spherical waves.

If the diffraction field in the hologram plane is spatially filtered, or if the diffusely scattering plane surface is transversally displaced, the interference pattern corresponding to Fig. 5b is located in the far diffraction zone. In this case, the difference between square radii of interference fringes in neighboring interference orders holds, when matte screen 1 (see Fig. 1) at the stage of hologram recording is illuminated by radiation with a spherical wave characterized by different values of the curvature radius and different signs. This follows from Eq. (18), in which the radii of interference fringes for fixed λ and Δl depend on the focal length f_1 . In addition, when the scatterer is illuminated by a

collimated beam, the spatial filtering of the diffraction field in the hologram plane is not necessary.

Consider the double-exposure recording of the hologram of a focused image to control for the transversal or longitudinal displacement of a diffusely scattering plane surface, taking into account that the field is diffraction-limited by the aperture diaphragms p_1, p_2 of, respectively, the lenses L_1, L_2 (Fig. 7).

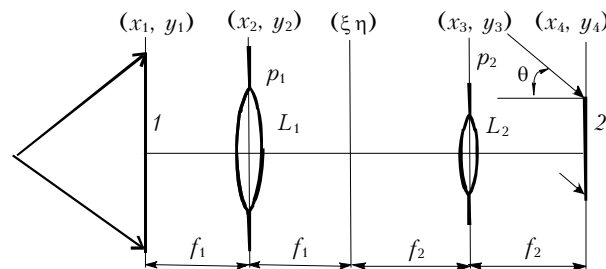


Fig. 7. Schematic of hologram recording for the focused image of a scatterer: matte screen 1; photographic plate 2; positive lenses L_1, L_2 ; aperture diaphragms p_1, p_2 .

Based on Refs. 8 and 9, the distribution of the field complex amplitude in the used parabolic approximation, corresponding to the first exposure, in the object channel in the plane (x_4, y_4) can be written in the form

$$u_1(x_4, y_4) \sim \left[\exp \frac{ik}{2f_2} (x_4^2 + y_4^2) \right] \left\{ \exp \left[-\frac{ik(x_4^2 + y_4^2)}{2f_2} \right] \times \int_{-\infty}^{\infty} \int_{-\infty}^{\infty} u_1(\xi, \eta) \exp[-ik(\xi x_4 + \eta y_4)/f_2] d\xi d\eta \otimes P_2(x_4, y_4) \right\}, \quad (21)$$

where $P_2(x_4, y_4)$ is the Fourier transform of $p_2(x_3, y_3)$ of the L_2 pupil with the spatial frequencies $x_4/\lambda f_2$ and $y_4/\lambda f_2$;

$$u_1(\xi, \eta) \sim \exp \left[\frac{ik(\xi^2 + \eta^2)}{2f_1} \right] \times \left\{ \exp \left[\frac{-ik(\xi^2 + \eta^2)}{2f_1} \right] \int_{-\infty}^{\infty} \int_{-\infty}^{\infty} t(x_1, y_1) \exp \left[\frac{ik}{2R} (x_1^2 + y_1^2) \right] \times \exp[-ik(x_1 \xi + y_1 \eta)/f_1] dx_1 dy_1 \otimes P_1(\xi, \eta) \right\}; \quad (22)$$

$P_1(\xi, \eta)$ is the Fourier transform of $p_1(x_2, y_2)$ of the lens L_1 pupil with the spatial frequencies $\xi/\lambda f_1$ and $\eta/\lambda f_1$.

If, as in Refs. 8 and 9, the phase change of a spherical wave with the curvature radius f_2 does not exceed π within the domain of existence of the function $P_2(x_4, y_4)$, then this condition is fulfilled in the plane (x_4, y_4) within the area of the diameter $D_2 \leq d_2$, where d_2 is the pupil diameter of the lens L_2 . Then after the substitution of Eq. (22) into Eq. (21) we obtain

$$\begin{aligned}
 u_1(x_4, y_4) \sim & P_2(x_4, y_4) \otimes \exp\left[-\frac{ik\mu(x_4^2 + y_4^2)}{2f_2}\right] \otimes \\
 & \otimes p_1(\mu x_4, \mu y_4) \left\{ \exp\left[\frac{ik\mu}{2f_2}(x_4^2 + y_4^2)\right] \otimes \right. \\
 & \left. \otimes t(-\mu x_4, -\mu y_4) \exp\left[\frac{ik\mu^2}{2R}(x_4^2 + y_4^2)\right] \right\}. \quad (23)
 \end{aligned}$$

In Eq. (23), we use the integral representation of the convolution operation, and thus it takes the form

$$\begin{aligned}
 u_1(x_4, y_4) \sim & P_2(x_4, y_4) \otimes \exp\left[-\frac{ik\mu(x_4^2 + y_4^2)}{2f_2}\right] \left\{ P_1(x_4, y_4) \otimes \right. \\
 & \left. \otimes \exp\left[\frac{ik\mu}{2f_2}(x_4^2 + y_4^2)\right] t(-\mu x_4, -\mu y_4) \exp\left[\frac{ik\mu^2}{2R}(x_4^2 + y_4^2)\right] \right\}, \quad (24)
 \end{aligned}$$

where $P_1(x_4, y_4)$ is the Fourier transform of the function $p_1(x_2, y_2)$ with the spatial frequencies $x_4/\lambda f_2$ and $y_4/\lambda f_2$.

If the phase change of the spherical wave with the curvature radius f_2/μ does not exceed π within the domain of existence of $P_1(x_4, y_4)$, then this condition is fulfilled in the plane (x_4, y_4) within the area of the diameter $D_1 \leq d_1/\mu$, where d_1 is the pupil diameter of the lens L_1 . Then the distribution of the complex amplitude of the field corresponding to the first exposure in the object channel in the plane of the photographic plate within the overlap of the areas indicated above is determined by the equation

$$\begin{aligned}
 u_1(x_4, y_4) \sim & t(-\mu x_4, -\mu y_4) \times \\
 & \times \exp\left[\frac{ik\mu^2}{2R}(x_4^2 + y_4^2)\right] \otimes P_1(x_4, y_4) \otimes P_2(x_4, y_4). \quad (25)
 \end{aligned}$$

Hence it follows that every point of the spatially limited image of the scatterer is extended up to the magnitude determined by the width of the function $P_1(x_4, y_4) \otimes P_2(x_4, y_4)$, corresponding to the subjective speckle size in the hologram plane.

When the matte screen t is displaced in the transversal direction before the second exposure (see Fig. 7), then the distribution of the complex amplitude of the field corresponding to the second exposure in the object channel in the plane (x_4, y_4) takes the form

$$\begin{aligned}
 u_2(x_4, y_4) \sim & \\
 \sim & \int_{-\infty}^{\infty} \int_{-\infty}^{\infty} u_2(\xi, \eta) \exp[-ik(\xi x_4 + \eta y_4)/f_2] d\xi d\eta \otimes P_2(x_4, y_4), \quad (26)
 \end{aligned}$$

where

$$\begin{aligned}
 u_2(\xi, \eta) \sim & \exp\left[\frac{ik(\xi^2 + \eta^2)}{2f_1}\right] \exp(ika\xi/f_1) \times \\
 & \times \left\{ \exp\left[\frac{-ik(\xi^2 + \eta^2)}{2f_1}\right] \left\{ F(\xi, \eta) \otimes \exp(-ika\xi/f_1) \times \right. \right. \\
 & \left. \left. \times \exp\left[\frac{-ikR(\xi^2 + \eta^2)}{2f_1^2}\right] \right\} \otimes \exp(-ika\xi/f_1) P_1(\xi, \eta) \right\}; \quad (27)
 \end{aligned}$$

$F(\xi, \eta)$ is the Fourier transform of $t(x_1, y_1)$ with the spatial frequencies $\xi/\lambda f_1$ and $\eta/\lambda f_1$.

The substitution of Eq. (27) into Eq. (26) yields

$$\begin{aligned}
 u_2(x_4, y_4) \sim & P_2(x_4, y_4) \otimes \exp\left\{-\frac{ik\mu}{2f_2}[(x_4 - a/\mu)^2 + y_4^2]\right\} \otimes \\
 & \otimes p_1(\mu x_4 + a, \mu y_4) \left\{ \exp\left[\frac{ik\mu}{2f_2}(x_4^2 + y_4^2)\right] \otimes \right. \\
 & \left. \otimes t(-\mu x_4, -\mu y_4) \exp\left[\frac{ik\mu^2}{2R}[(x_4 + a/\mu)^2 + y_4^2]\right] \right\}.
 \end{aligned}$$

Since, for example¹⁰:

$$\exp\left[\frac{ik\mu}{2f_2}(x_4^2 + y_4^2)\right] \otimes \exp\left[-\frac{ik\mu}{2f_2}(x_4^2 + y_4^2)\right] = \delta(x_4, y_4),$$

where $\delta(x_4, y_4)$ is the Dirac's delta, the integral representation of the convolution operation ensures the possibility to prove that the following identities are fulfilled:

$$\begin{aligned}
 & \exp\left\{-\frac{ik\mu}{2f_2}[(x_4 - a/\mu)^2 + y_4^2]\right\} \otimes \\
 & \otimes \exp\left[\frac{ik\mu}{2f_2}(x_4^2 + y_4^2)\right] \otimes P_2(x_4, y_4) = P_2(x_4 - a/\mu, y_4), \quad (28)
 \end{aligned}$$

$$\begin{aligned}
 & \exp\left[-\frac{ik\mu}{2f_2}(x_4^2 + y_4^2)\right] \otimes p_1(\mu x_4 + a, \mu y_4) \times \\
 & \times \left\{ \exp\left[\frac{ik\mu}{2f_2}(x_4^2 + y_4^2)\right] \otimes t(-\mu x_4, -\mu y_4) \times \right. \\
 & \left. \times \exp\left\{\frac{ik\mu^2}{2R}[(x_4 + a/\mu)^2 + y_4^2]\right\} \right\} = \\
 & = \exp\left\{-\frac{ik\mu}{2f_2}[(x_4 + a)^2 + y_4^2]\right\} \times \\
 & \times \left\{ P_1(x_4, y_4) \otimes \exp\left\{\frac{ik\mu}{2f_2}[(x_4 + a)^2 + y_4^2]\right\} \times \right. \\
 & \left. \times t(-\mu x_4, -\mu y_4) \exp\left\{\frac{ik\mu^2}{2R}[(x_4 + a/\mu)^2 + y_4^2]\right\} \right\}. \quad (29)
 \end{aligned}$$

Based on them, the distribution of the complex amplitude of the field corresponding to the second

exposure in the object channel in the plane (x_4, y_4) within the overlap of the areas with the diameters D_1 and D_2 is determined by the equation

$$u_2(x_4, y_4) \sim t(-\mu x_4, -\mu y_4) \exp\left\{\frac{ik\mu^2}{2R}[(x_4 + a/\mu)^2 + y_4^2]\right\} \otimes P_1(x_4, y_4) \otimes P_2(x_4 - a/\mu, y_4). \quad (30)$$

Here it is taken into account the a is small. If the double-exposure hologram is recorded at the linear part of the photomaterial blackening curve, then based on Eqs. (25) and (30) the distribution of the complex amplitude of transmittance corresponding to the (-1) -st diffraction order takes the form

$$\begin{aligned} \tau(x_4, y_4) \sim & \exp(-ikx_4 \sin\theta) \{t(-\mu x_4, -\mu y_4) \times \\ & \times \exp\left[\frac{ik\mu^2}{2R}(x_4^2 + y_4^2)\right] \otimes P_1(x_4, y_4) \otimes P_2(x_4, y_4) + \\ & + t(-\mu x_4, -\mu y_4) \exp\left[\frac{ik\mu^2}{2R}[(x_4 + a/\mu)^2 + y_4^2]\right] \otimes \\ & \otimes P_1(x_4, y_4) \otimes P_2(x_4 - a/\mu, y_4)\}. \end{aligned} \quad (31)$$

It follows from Eq. (31) that, in the hologram plane, subjective speckles corresponding to the second exposure are shifted in the direction opposite to the direction of the scatterer movement. In addition, they are sloped with respect to identical speckles corresponding to the first exposure, and the sign of the slope angle alternates, when the matte screen 1 (see Fig. 7) is illuminated by the coherent radiation with the convergent spherical wave.

If the diffraction field is spatially filtered at the stage of hologram reconstruction in the hologram plane on the optical axis according to Fig. 2 (hereinafter one should take into account the replacement in the designations of the planes: (x_3, y_3) by (x_4, y_4) and (x_4, y_4) by (x_5, y_5)) and the phase change $k\mu a x_4/R$ does not exceed π within the filtering aperture, then the distribution of the complex amplitude of the field at the output of the spatial filter is determined by the equation

$$\begin{aligned} u(x_4, y_4) \sim & p_0(x_4, y_4) \left\{ t(-\mu x_4, -\mu y_4) \exp\left[\frac{ik\mu^2}{2R}(x_4^2 + y_4^2)\right] \otimes \right. \\ & \otimes P_1(x_4, y_4) \otimes P_2(x_4, y_4) + \exp\left(\frac{ika^2}{2R}\right) t(-\mu x_4, -\mu y_4) \times \\ & \times \exp\left[\frac{ik\mu^2}{2R}(x_4^2 + y_4^2)\right] \otimes \exp(-ik\mu a x_4/R) \times \\ & \left. \times P_1(x_4, y_4) \otimes \exp(-ik\mu a x_4/R) P_2(x_4 - a/\mu, y_4) \right\}. \end{aligned} \quad (32)$$

Based on Eq. (32), once the Fourier transform is performed to obtain the distribution of the complex

amplitude of the field in the back focal plane of the lens L_3 (see Fig. 2) with the focal length $f_3 = f_2$, the illumination distribution in this plane within the overlap of the functions

$$p_1(x_5, y_5) p_2(x_5, y_5), p_1\left(x_5 + a\frac{f_1}{R}, y_5\right) p_2\left(x_5 + a\frac{f_1}{R}, y_5\right)$$

takes the form

$$\begin{aligned} I(x_5, y_5) \sim & \left[1 + \cos\left(\frac{ka^2}{2R} + \frac{kax_5}{f_1}\right)\right] \times \\ & \times \left| p_1(x_5, y_5) p_2(x_5, y_5) \left\{ F(x_5, y_5) \otimes \exp\left[-\frac{ikR}{2f_1^2}(x_5^2 + y_5^2)\right] \right\} \otimes \right. \\ & \left. \otimes P_0(x_5, y_5) \right|^2, \end{aligned} \quad (33)$$

where $F(x_5, y_5)$ is the Fourier transform of the function $t(-\mu x_4, -\mu y_4)$ with the spatial frequencies $x_5/\lambda f_2$ and $y_5/\lambda f_2$.

It follows from Eq. (33) that, taking into account that the pupil images of L_1 and L_2 displace only slightly (see Fig. 7), the subjective speckle structure is modulated within the overlap of $p_1(x_5, y_5)$ and $p_2(x_5, y_5)$ by interference fringes, changing on the axis x , with the repetition period $\Delta x_5 = \lambda f_1/a$, which is independent of the curvature radius of the spherical wave of radiation used to illuminate the scatterer at the stage of hologram recording.

If at the stage of hologram reconstruction the spatial filtering of the diffraction field is performed on the optical axis in the Fourier plane (see Fig. 3) (hereinafter one should take into account the replacement in the designations of the planes: (x_3, y_3) by (x_4, y_4) , (x_4, y_4) by (x_5, y_5) , and (x_5, y_5) by (x_6, y_6)) and the phase change $ka x_4/f_1$ does not exceed π within the filtering aperture, then, provided that the field is not spatially limited due to the finite aperture of the lens L_3 , the distribution of its complex amplitude at the output of the filtering aperture is determined by the equation

$$\begin{aligned} u(x_5, y_5) \sim & p_0(x_5, y_5) \times \\ & \times \left\{ F(x_5, y_5) \otimes \exp\left[-\frac{ikR}{2f_1^2}(x_5^2 + y_5^2)\right] + F(x_5, y_5) \otimes \right. \\ & \left. \otimes \exp(ika x_5/f_1) \exp\left[-\frac{ikR}{2f_1^2}(x_5^2 + y_5^2)\right] \right\}, \end{aligned} \quad (34)$$

where $p_0(x_5, y_5)$ is the transmission function of the spatial filter.

Based on Eq. (34), once the Fourier transform is performed to obtain the distribution of the complex amplitude of the field in the plane of formation of the hologram image, for the focal length f_4 of the lens L_4 (see Fig. 3) equal to f_2 , the illumination distribution in this plane takes the form

$$I(x_6, y_6) \sim \left[1 + \cos\left(\frac{ka^2}{2R} - \frac{k\mu}{R}ax_6\right) \right] \times \left| t(\mu x_6, \mu y_6) \exp\left[\frac{ik\mu^2}{2R}(x_6^2 + y_6^2)\right] \otimes P_0(x_6, y_6) \right|^2, \quad (35)$$

where $P_0(x_6, y_6)$ is the Fourier transform of the transmission function $p_0(x_5, y_5)$ of the spatial filter with the spatial frequencies $x_6/\lambda f_2, y_6/\lambda f_2$.

According to Eq. (35), within the spatially limited (in the case under consideration) scatterer image, the interference pattern in the form of interference fringes, periodically intermittent on the x axis, modulates the subjective speckle structure. The period $\Delta x_6 = \lambda|R|/\mu a$ of interference fringes depends on the magnification of the two-component optical system in Fig. 7 and on the curvature radius R of the spherical wave of coherent radiation used to illuminate the scatterer at the stage of hologram recording. In addition, as in the case of image formation for the diffusely scattering plane surface, according to Fig. 1, the interferometer sensitivity is independent of the sign of the curvature radius, and at $R = \infty$ "frozen" interference fringes are formed in the far diffraction zone. The recording of these fringes in the Fourier plane does not require the spatial filtering of the diffraction field.

Let the matte screen 1 (see Fig. 7) turn out to be displaced by $\Delta l = f'_1 - f_1$ along the z axis before the second exposure. Then in the approximation used, the distribution of the complex amplitude of the field corresponding to the second exposure in the frequency plane (ξ, η) (see Fig. 7) is determined by the equation

$$u'_2(\xi, \eta) \sim \exp(ik\Delta l) \exp\left[\frac{ik}{2f_1}(\xi^2 + \eta^2)\right] \times \left\{ \exp\left[-\frac{ik(f_1 + \Delta l)}{2f_1^2}(\xi^2 + \eta^2)\right] \times \left\{ F(\xi, \eta) \otimes \exp\left[-\frac{ik(R - \Delta l)}{2f_1^2}(\xi^2 + \eta^2)\right] \right\} \otimes P_1(\xi, \eta) \right\}. \quad (36)$$

Since within the subjective speckle in the plane (ξ, η) , determined by the width of the function $P_1(\xi, \eta)$ equal to $\approx \lambda f_1/d_1$, the phase change of the spherical wave with the curvature radius $f_1^2/\Delta l$ does not exceed π within the area $d_1 f_1/\Delta l$, whose diameter far exceeds d_1 for $\Delta l \ll f_1$, in Eq. (36) the factor $\exp[-ik\Delta l(\xi^2 + \eta^2)/2f_1^2]$ can be taken off the convolution integral. Then the substitution of Eq. (36) in Eq. (21) for $u_1(\xi, \eta)$ yields the distribution of the complex amplitude of the field in the plane (x_4, y_4) within the area of diameter D_2 in the form

$$u'_2(x_4, y_4) \sim P_2(x_4, y_4) \otimes \exp\left[\frac{ik\mu^2}{2\Delta l}(x_4^2 + y_4^2)\right] \otimes \exp\left[-\frac{ik\mu}{2f_2}(x_4^2 + y_4^2)\right] \otimes p_1(\mu x_4, \mu y_4) \left\{ \exp\left[\frac{ik\mu}{2f_2}(x_4^2 + y_4^2)\right] \otimes t(-\mu x_4, -\mu y_4) \exp\left[\frac{ik\mu^2}{2(R - \Delta l)}(x_4^2 + y_4^2)\right] \right\} \exp(ik\Delta l). \quad (37)$$

In its turn, based on the integral representation of the convolution operation in Eq. (37), the distribution of the complex amplitude of the field corresponding to the second exposure in the object channel in the plane of the photographic plate 2 (see Fig. 7) within the overlap of the areas with diameters D_1 and D_2 is determined by the equation

$$u'_2(x_4, y_4) \sim \exp(ik\Delta l) t(-\mu x_4, -\mu y_4) \exp\left[\frac{ik\mu^2(x_4^2 + y_4^2)}{2(R - \Delta l)}\right] \otimes \exp\left[\frac{ik\mu^2}{2\Delta l}(x_4^2 + y_4^2)\right] \otimes P_1(x_4, y_4) \otimes P_2(x_4, y_4). \quad (38)$$

If the double-exposure hologram recording is performed on the linear part of the photomaterial blackening curve, the distribution of the complex amplitude of the hologram transmittance corresponding to the (-1) -st diffraction order for $\Delta l \ll R$ based on Eqs. (25) and (38) takes the form

$$\tau'(x_4, y_4) \sim \exp(-ikx_4 \sin\theta) \times \left\{ t(-\mu x_4, -\mu y_4) \exp\left[\frac{ik\mu^2(x_4^2 + y_4^2)}{2R}\right] \otimes P_1(x_4, y_4) \otimes P_2(x_4, y_4) + \exp(ik\Delta l) t(-\mu x_4, -\mu y_4) \times \exp\left[\frac{ik\mu^2(x_4^2 + y_4^2)}{2R}\right] \exp\left[\frac{ik\mu^2\Delta l(x_4^2 + y_4^2)}{2R^2}\right] \otimes \exp\left[\frac{ik\mu^2(x_4^2 + y_4^2)}{2\Delta l}\right] \otimes P_1(x_4, y_4) \otimes P_2(x_4, y_4) \right\}. \quad (39)$$

It follows from Eq. (39) that subjective speckles of the two exposures coincide in the hologram. The speckles corresponding to the second exposure are extended up to

$$P_1(x_4, y_4) \otimes P_2(x_4, y_4) \otimes \left[\exp\frac{ik\mu^2}{2\Delta l}(x_4^2 + y_4^2) \right].$$

In addition, in the hologram plane the slope angle of speckles corresponding to the second exposure changes along the radius from the optical axis, and the sign of the slope angle, depending on μ and R , changes to the opposite one as the matte

screen 1 (see Fig. 7) is illuminated by the radiation with the convergent spherical wave.

If at the stage of hologram reconstruction (according to Fig. 2) the spatial filtering of the diffraction field is performed in the hologram plane on the optical axis and the phase change $k\mu^2\Delta l(x_4^2 + y_4^2)/2R^2$ does not exceed π within the filtering aperture, then the distribution of the complex amplitude of the field at the output of the spatial filter is determined by the equation

$$u'(x_4, y_4) \sim p_0(x_4, y_4) \left\{ t(-\mu x_4, -\mu y_4) \exp \left[\frac{ik\mu^2}{2R} (x_4^2 + y_4^2) \right] \otimes \right. \\ \left. \otimes P_1(x_4, y_4) \otimes P_2(x_4, y_4) \left\{ 1 + \exp(ik\Delta l) \exp \left[\frac{ik\mu^2}{2\Delta l} (x_4^2 + y_4^2) \right] \right\} \right\}. \quad (40)$$

Based on this equation, once the Fourier transform is applied to determine the distribution of the complex amplitude of the field in the back focal plane of the lens L_3 (see Fig. 2) with the focal length $f_3 = f_2$, the illumination distribution in this plane takes the form

$$I'(x_5, y_5) \sim \left\{ 1 + \cos \left[k\Delta l - \frac{k\Delta l(x_5^2 + y_5^2)}{2f_1^2} \right] \right\} \times \\ \times \left| p_1(x_5, y_5) p_2(x_5, y_5) \left\{ F(x_5, y_5) \otimes \exp \left[-\frac{ikR}{2f_1^2} (x_5^2 + y_5^2) \right] \right\} \otimes \right. \\ \left. \otimes P_0(x_5, y_5) \right|^2. \quad (41)$$

It follows from Eq. (41) that within the overlap of the pupil images of L_1 and L_2 (see Fig. 7) the subjective speckle structure is modulated by fringes of an equal slope – a system of concentric rings. The ring radii are independent of the curvature radius of the spherical wave of radiation used to illuminate the scatterer at the stage of hologram recording.

If at this stage the spatial filtering of the diffraction field is performed on the optical axis in the Fourier plane (see Fig. 3) and the phase change $k\Delta l(x_5^2 + y_5^2)/2f_1^2$ does not exceed π within the filtering aperture, then, provided that the field is not spatially limited due to the finite size of the aperture of the lens L_3 , the distribution of the complex amplitude of the field at the output of the filtering aperture is determined by the equation

$$u'(x_5, y_5) \sim p_0(x_5, y_5) \left\{ F(x_5, y_5) \otimes \exp \left[-\frac{ikR}{2f_1} (x_5^2 + y_5^2) \right] + \right. \\ \left. + \exp(ik\Delta l) F(x_5, y_5) \otimes \exp \left[-\frac{ik(R-\Delta l)}{2f_1^2} (x_5^2 + y_5^2) \right] \right\}. \quad (42)$$

Then after the Fourier transform, believing that the focal length of L_4 (see Fig. 3) is equal to f_2 , based on the thus obtained distribution of the complex amplitude of the field in the plane of formation of the hologram image, the illumination distribution in this plane takes the form

$$I'(x_6, y_6) \sim \left\{ 1 + \cos \left[k\Delta l + \frac{k\mu^2\Delta l(x_6^2 + y_6^2)}{2R^2} \right] \right\} \times \\ \times \left| t(\mu x_6, \mu y_6) \exp \left[\frac{ik\mu^2(x_6^2 + y_6^2)}{2R} \right] \otimes P_0(x_6, y_6) \right|^2. \quad (43)$$

According to Eq. (43), in the recording plane 3 (see Fig. 3) the interference pattern in the form of equal-slope fringes modulates the subjective speckle structure with the speckle size determined by the width of the function $P_0(x_6, y_6)$ within the spatially limited (in the case considered) scatterer image. In this case, the radii of interference fringes depend on μ and R . In addition, at $R = \infty$ “frozen” interference fringes (concentric rings) are formed in the far diffraction zone. The recording of these fringes in the Fourier plane does not require the spatial filtering of the diffraction field in the hologram plane.

The above analysis of formation of the interference patterns characterizing the transversal or longitudinal displacement of a diffusely scattering plane surface shows that these patterns are located in two planes, which leads to the different sensitivity of the interferometer. On the one hand, the interference pattern is located in the far diffraction zone (Fourier plane), where identical speckles of the two exposures coincide. On the other hand, subjective speckles corresponding to the second exposure are sloped relative to speckles of the first exposure in the hologram plane; and this slope is constant in the case of the transversal displacement of the scatterer and varying along the radius from the optical axis in the case of the longitudinal displacement. Due to this, the interference patterns are located in the hologram plane. As a result, only the spatial filtering of the diffraction field in the corresponding planes of location can provide for the unambiguous determination of the interferometer sensitivity to a scatterer displacement.

In the experiment, the pupil diameters of L_1 and L_2 (see Fig. 7), used to form the image of the matte screen 1, made 25 mm, and the fixed transversal and longitudinal displacements of the scatterer before the second exposure of the photographic plate were equal to $a = (0.03 \pm 0.002)$ mm and $\Delta l = (2 \pm 0.002)$ mm.

As an example, Figure 8a shows the interference pattern located in the Fourier plane and characterizing the transversal displacement of the matte screen. This pattern was recorded, when the hologram was reconstructed on the optical axis with the aid of a small aperture (≈ 2 mm) laser beam. The

lateral surface of L_1 was marked as 1 on the left, while the lateral surface of L_2 was marked as 2 on the right (Fig. 8).

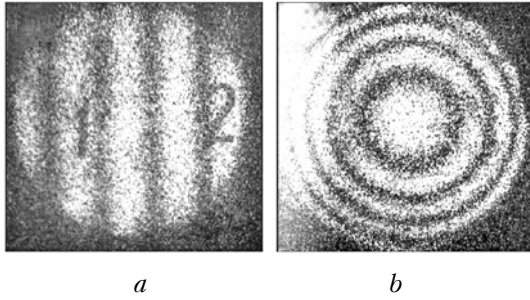


Fig. 8. Interference patterns located in the Fourier plane and characterizing the transversal (*a*) and longitudinal (*b*) displacements of the scatterer.

The frequency of interference fringes remained unchanged at changes of both the value and the sign of the curvature radius of the spherical wave of the coherent radiation used to illuminate the scatterer at the stage of hologram recording. The transversal displacement $a = \lambda f_1 / \Delta x_5$ of the matte screen determined from the measurements of the period Δx_5 of interference fringes was in agreement with the value indicated above accurate to the experimental error (10%). Taking into account that the scatterer image is spatially limited, the spatial filtering of the diffraction field in the hologram plane off the optical axis, when the center of the filtering aperture has the coordinates x_{04} and 0, leads to the distribution of the complex amplitude of the field at the output of the spatial filter in the form

$$\begin{aligned}
 u(x_4, y_4) \sim & p_0(x_4, y_4) \left\{ t(-\mu x_4 - \mu x_{04}, -\mu y_4) \times \right. \\
 & \times \exp \left\{ \frac{ik\mu^2}{2R} [(x_4 + x_{04})^2 + y_4^2] \right\} \otimes \exp(-ikx_{04}x_4/f_2) \times \\
 & \times P_1(x_4, y_4) \otimes \exp(ikx_{04}x_4/f_2) P_2(x_4, y_4) + \\
 & + \exp(ika^2/2R) \exp(ik\mu a x_{04}/R) t(-\mu x_4 - \mu x_{04}, -\mu y_4) \times \\
 & \times \exp \left\{ \frac{ik\mu^2}{2R} [(x_4 + x_{04})^2 + y_4^2] \right\} \otimes \exp(-ik\mu a x_4/R) \times \\
 & \times \exp(-ikx_{04}x_4/f_2) P_1(x_4, y_4) \otimes \exp(-ik\mu a x_4/R) \times \\
 & \left. \times \exp(ikx_{04}x_4/f_2) P_2(x_4, y_4) \right\}. \quad (44)
 \end{aligned}$$

Consequently, in the back focal plane of L_3 (see Fig. 2), the distribution of the complex amplitude of the field is determined by the equation

$$\begin{aligned}
 u(x_5, y_5) \sim & \left\{ \left\{ F(x_5, y_5) \exp(-ik\mu x_{04}x_5/f_2) \otimes \right. \right. \\
 & \left. \left. \otimes \exp \left[-\frac{ikR}{2f_1^2} (x_5^2 + y_5^2) \right] \exp(ikx_{04}x_5/f_2) \right\} \times \right. \\
 & \times \left\{ p_1(x_5 + x_{04}, y_5) p_2(x_5 - x_{04}, y_5) + p_1 \left(x_5 + x_{04} + \frac{f_1}{R} a, y_5 \right) \times \right. \\
 & \left. \left. \times p_2 \left(x_5 - x_{04} + \frac{f_1}{R} a, y_5 \right) \exp \left[i \left(\frac{ka^2}{R} - \frac{k\mu a x_{04}}{R} + \frac{kax_5}{f_1} \right) \right] \right\} \right\} \otimes \\
 & \otimes P_0(x_5, y_5). \quad (45)
 \end{aligned}$$

If in Eq. (45) the period of variation of $1 + \exp(ikax_5/f_1)$ exceeds at least tenfold the width of $P_0(x_5, y_5)$, which determines the size of a subjective speckle in the Fourier plane, then, taking into account that af_1/R is small, the illumination distribution in the Fourier plane takes the form

$$\begin{aligned}
 I(x_5, y_5) \sim & \left[1 + \cos \left(\frac{ka^2}{2R} - \frac{k\mu a x_{04}}{R} + \frac{kax_5}{f_1} \right) \right] \times \\
 & \times \left| p_1(x_5 + x_{04}, y_5) p_2(x_5 - x_{04}, y_5) \times \right. \\
 & \left. \times \left\{ F(x_5, y_5) \exp(-ik\mu x_{04}x_5/f_2) \otimes \right. \right. \\
 & \left. \left. \otimes \exp \left[-\frac{ikR}{2f_1^2} (x_5^2 + y_5^2) \right] \exp(ikx_{04}x_5/f_2) \right\} \otimes P_0(x_5, y_5) \right|^2. \quad (46)
 \end{aligned}$$

It follows from Eq. (46) that within the overlap of the pupil images of L_1 and L_2 the subjective speckle structure is modulated by interference fringes periodically intermittent on the x axis. The behavior of interference fringes upon the displacement of the filtering aperture on the axis x is similar to that taking place in the case of the scatterer image formation according to Fig. 1. In addition, the parallax of interference fringes is observed in both cases, as follows from the form of Eq. (46).

Interference fringes in Fig. 9 characterize the transversal displacement of the scatterer and lie in the hologram plane.

Their recording was conducted when spatially filtering the diffraction field on the optical axis in the Fourier plane with the filtering aperture 2 mm in diameter. Figure 9a corresponds to the case that the matte screen 1 (see Fig. 7) was illuminated by the coherent radiation with the divergent spherical wave having curvature radius $R = 200$ mm, whereas Figure 9b corresponds to the convergent wave with $R = 330$ mm.

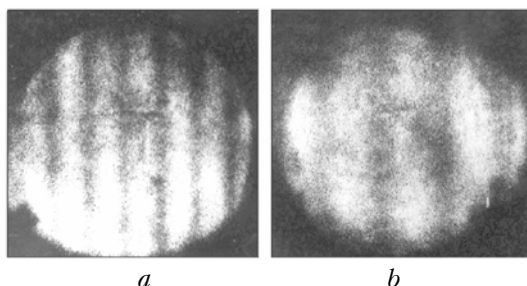


Fig. 9. Interference patterns: the screen was illuminated by radiation with the divergent (a) and convergent (b) spherical waves.

The periods of interference fringes were measured in these two cases, as well as in others connected with the changed value and sign of the curvature radius. The measured values coincided with $\Delta x_6 = \lambda|R|/\mu a$ accurate to the experimental error (10%).

To analyze the spatial filtering of the diffraction field in the Fourier plane off the optical axis, it is necessary to determine the field distribution in this plane provided that the field is not diffraction-limited due to the finite size of the L_3 aperture (see Fig. 3). Based on Eq. (21) we obtain

$$u_1(x_5, y_5) \sim \exp\left[-\frac{ik}{2f_2}(x_5^2 + y_5^2)\right] \otimes p_2(x_5, y_5) \left\{ \exp\left[\frac{ik}{2f_2}(x_5^2 + y_5^2)\right] \otimes g(x_5, y_5) \right\}, \quad (47)$$

where

$$g(x_5, y_5) \sim \exp\left[\frac{ik}{2f_1}(x_5^2 + y_5^2)\right] \left\{ \exp\left[-\frac{ik}{2f_1}(x_5^2 + y_5^2)\right] \times \left[F'(-x_5, -y_5) \otimes \exp\left[-\frac{ikR}{2f_1^2}(x_5^2 + y_5^2)\right] \right] \otimes P_1'(x_5, y_5) \right\};$$

$F'(x_5, y_5)$, $P_1'(x_5, y_5)$ are the Fourier transforms of, respectively, the functions $t(x_1, y_1)$ and $p_1(x_2, y_2)$ with the spatial frequencies $x_5/\lambda f_1$ and $y_5/\lambda f_1$. Then, using the above analysis of formation of subjective speckles in the optical system considered, we can show that the distribution of the complex amplitude of the field in the Fourier plane corresponding to the first exposure within the overlap of the areas with the diameters $D_1' \leq d_1$, $D_2' \leq d_2$ takes the form

$$u_1(x_5, y_5) \sim F'(-x_5, -y_5) \otimes \exp\left[-\frac{ikR}{2f_1^2}(x_5^2 + y_5^2)\right] \otimes P_1'(x_5, y_5) \otimes P_2(x_5, y_5). \quad (48)$$

In its turn, the distribution of the complex amplitude corresponding to the second exposure is determined by the equation

$$u_2(x_5, y_5) \sim \exp(-ika x_5/f_1) \left\{ F'(-x_5, -y_5) \otimes \exp(ika x_5/f_1) \times \left[\exp\left[-\frac{ikR}{2f_1^2}(x_5^2 + y_5^2)\right] \otimes P_1'(x_5, y_5) \otimes P_2(x_5, y_5) \right] \right\}. \quad (49)$$

If the filtering aperture center has coordinates x_{05} and 0, then based on Eqs. (48) and (49), the distribution of the complex amplitude of the field at the output of the spatial filter takes the form

$$u(x_5, y_5) \sim p_0(x_5, y_5) \left\{ F'(-x_5 - x_{05}, -y_5) \otimes \exp\left[-\frac{ikR}{2f_1^2}[(x_5 + x_{05})^2 + y_5^2]\right] \otimes \exp(-ikx_{05}x_5/f_1) \times \left[P_1'(x_5, y_5) \otimes \exp(ikx_{05}x_5/f_2) P_2(x_5, y_5) + \exp(-ika x_{05}/f_1) F'(-x_5 - x_{05}, -y_5) \right] \otimes \exp\left[-\frac{ikR}{2f_1^2}[(x_5 + x_{05})^2 + y_5^2]\right] \exp(-ika x_5/f_1) \otimes \exp(-ikx_{05}x_5/f_1) \exp(ika x_5/f_1) \times \left[P_1'(x_5, y_5) \otimes \exp(ikx_{05}x_5/f_2) \exp(ika x_5/f_1) P_2(x_5, y_5) \right] \right\}. \quad (50)$$

Based on this equation and taking into account that af_2/f_1 is small compared to x_{05} (in the pupil function), the illumination distribution in the plane of formation of the hologram image is determined by the equation

$$I(x_6, y_6) \sim \left[1 + \cos\left(\frac{ka^2}{2R} - \frac{kx_{05}x_6}{f_1} - \frac{k\mu ax_6}{R}\right) \right] \times \left| p_1(\mu x_6 + x_{05}, \mu y_6) p_2(x_6 - x_{05}, y_6) t(\mu x_6, \mu y_6) \times \exp\left[\frac{ik\mu^2}{2R}(x_6^2 + y_6^2)\right] \otimes P_0(x_6, y_6) \right|^2. \quad (51)$$

According to Eq. (51), within the overlap of the functions $p_1(\mu x_6 + x_{05}, \mu y_6)$, $p_2(x_6 - x_{05}, y_6)$, limiting the size of the scatterer image in the plane of hologram formation, the subjective speckle structure is modulated by interference fringes shifted periodically on the x axis. As the center of the filtering aperture shifts along the x axis, the behavior of interference fringes is similar to that taking place in the case of scatterer image formation at hologram recording in Fig. 1. In addition, the parallax of interference fringes is observed in the both cases, as follows from the form of Eq. (51).

The interference pattern (see Fig. 8b) characterizing the longitudinal displacement of the scatterer and located in the Fourier plane was recorded upon the reconstruction of the double-exposure hologram on the optical axis by a small

aperture (≈ 2 mm) laser beam. In this case, the difference of the square radii of interference fringes in the neighboring interference orders conserves, when at the stage of hologram recording the matte screen 1 (see Fig. 7) is illuminated by radiation with the spherical wave having the curvature radius of different sign and different value, as follows from Eq. (41), in which the radii of interference fringes depend on the focal length f_1 for fixed λ and Δl . In addition, if the scatterer was illuminated by a collimated beam, the spatial filtering of the diffraction field in the hologram plane was not necessary.

In the general case of spatial filtering performed off the optical axis, for example, the center of the filtering aperture lies at a point with coordinates $x_{04}, 0$ and the phase change $k\mu^2\Delta l x_4^2/2R^2$ does not exceed π within the filtering aperture, then the distribution of the complex amplitude of the field at the output of the spatial filter takes the form

$$\begin{aligned}
 u'(x_4, y_4) \sim & p_0(x_4, y_4) \left\{ t(-\mu x_4 - \mu x_{04}, -\mu y_4) \times \right. \\
 & \times \exp\left\{ \frac{ik\mu^2}{2R} [(x_4 + x_{04})^2 + y_4^2] \right\} \otimes \\
 & \otimes \exp(-ikx_{04} x_4/f_2) P_1(x_4, y_4) \otimes \exp(ikx_{04} x_4/f_2) P_2(x_4, y_4) \times \\
 & \left. \times \left\{ 1 + \exp(ik\Delta l) \exp(ik\mu^2\Delta l x_{04}^2/2R^2) \exp\left[\frac{ik\mu^2}{2\Delta l} (x_4^2 + y_4^2) \right] \right\} \right\}.
 \end{aligned} \tag{52}$$

Consequently, as a result of the Fourier transform performed to determine the distribution of the complex amplitude of the field in the back focal plane of the positive lens with the focal length equal to f_2 , the illumination distribution in this plane is determined by the following equation:

$$\begin{aligned}
 I'(x_5, y_5) \sim & \left\{ 1 + \cos\left[k\Delta l + \frac{k\mu^2\Delta l x_{04}^2}{2R^2} - \frac{k\Delta l(x_5^2 + y_5^2)}{2f_1^2} \right] \right\} \times \\
 & \times \left| p_1(x_5 + x_{04}, y_5) p_2(x_5 - x_{04}, y_5) \times \right. \\
 & \times \left. \left\{ \exp(-ik\mu x_{04} x_5/f_2) F(x_5, y_5) \otimes \right. \right. \\
 & \left. \left. \otimes \exp(ikx_{04} x_5/f_2) \exp\left[-\frac{ikR}{2f_1^2} (x_5^2 + y_5^2) \right] \right\} \otimes P_0(x_5, y_5) \right|^2.
 \end{aligned} \tag{53}$$

According to Eq. (53) within the overlap of the pupil images $p_1(x_5 + x_{04}, y_5)$ and $p_2(x_5 - x_{04}, y_5)$ (Fig. 10a for $\Delta x_4 = 4$ mm) the subjective speckle

structure is modulated by fringes of equal slope — a system of concentric rings. As the center of the filtering aperture shifts along the x axis, the behavior of these fringes is similar to that taking place in the case of scatterer image formation at hologram recording in Fig. 1. In addition, the parallax of interference fringes is absent in the both cases, as follows from Eqs. (18), (53), and Fig. 10a.

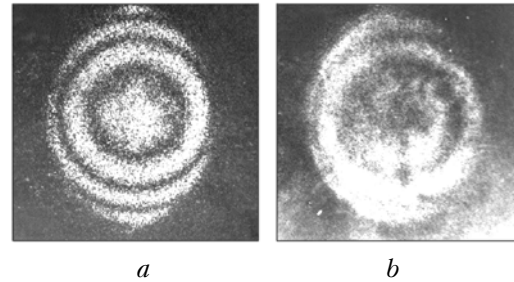


Fig. 10. Interference patterns characterizing the longitudinal displacement of the scatterer and recorded with the spatial filtering of the diffraction field performed off the optical axis: (a) in the Fourier plane and (b) in the plane of formation of the hologram image.

The interference patterns in Fig. 11 characterize the longitudinal displacement of the diffusely scattering plane surface and lie in the hologram plane. They were recorded with the spatial filtering of the diffraction field performed on the optical axis in the Fourier plane with a filtering aperture of 2 mm in diameter.

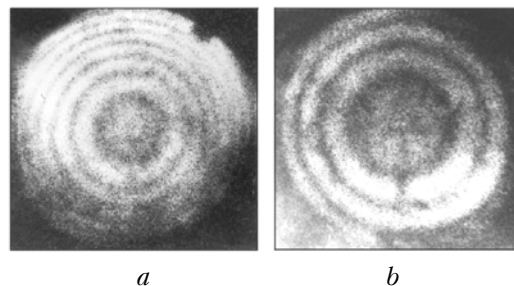


Fig. 11. Interference fringes: screen was illuminated by radiation with the divergent (a) and convergent (b) spherical waves.

Figure 11a corresponds to the case that the matte screen (see Fig. 7) is illuminated by the coherent radiation with the divergent spherical wave having the curvature radius $R = 200$ mm, while Figure 11b corresponds to the case of the convergent spherical wave with $R = 330$ mm. In these two cases and in others associated with the change in the value and sign of the curvature radius, we measured the radii of interference fringes in neighboring interference orders and determined the longitudinal displacement of the scatterer from the measured values and known λ , μ , and $|R|$ using Eq. (43). The displacement obtained coincides with $\Delta l = 2$ mm

indicated above accurate to the experimental error (10%).

In a more general case of the spatial filtering performed off the optical axis taking into account the distribution of the complex amplitude of the field corresponding to the first exposure [Eq. (48)] in the Fourier plane, for the second exposure:

$$u'_2(x_5, y_5) \sim \exp(ik\Delta l) \left\{ F'(-x_5, -y_5) \otimes \exp \left[-\frac{ik(R-\Delta l)}{2f_1^2} (x_5^2 + y_5^2) \right] \otimes P_1(x_5, y_5) \otimes P_2(x_5, y_5) \right\} \times \exp \left[-\frac{ik\Delta l}{2f_1^2} (x_5^2 + y_5^2) \right], \quad (54)$$

the distribution of the complex amplitude of the field at the output of the filtering aperture, whose center lies, for example, at a point with coordinates $x_{05}, 0$ and within which the phase change $k\Delta l x_5^2 / 2f_1^2$ does not exceed π , takes the form

$$u'(x_5, y_5) \sim p_0(x_5, y_5) \left\{ F'(-x_5 - x_{05}, -y_5) \otimes \exp \left\{ -\frac{ikR}{2f_1^2} [(x_5 + x_{05})^2 + y_5^2] \right\} \otimes \exp(-ikx_{05}x_5/f_1) \times P_1(x_5, y_5) \otimes \exp(ikx_{05}x_5/f_2) P_2(x_5, y_5) + \exp(ik\Delta l) \exp \left(-\frac{ik\Delta l x_{05}^2}{2f_1^2} \right) F'(-x_5 - x_{05}, -y_5) \otimes \exp \left\{ -\frac{ik(R-\Delta l)}{2f_1^2} [(x_5 + x_{05})^2 + y_5^2] \right\} \otimes \exp(-ikx_{05}x_5/f_1) \times P_1(x_5, y_5) \otimes \exp(ikx_{05}x_5/f_2) P_2(x_5, y_5) \right\}. \quad (55)$$

Consequently, once the Fourier transform is performed to obtain the distribution of the complex amplitude of the field in the back focal plane of the positive lens with the focal length f_2 , the illumination distribution in this plane is determined by the equation

$$I'(x_6, y_6) \sim \left\{ 1 + \cos \left[k\Delta l - \frac{k\Delta l x_{05}^2}{2f_1^2} + \frac{k\mu^2 \Delta l (x_6^2 + y_6^2)}{2R^2} \right] \right\} \times \left| p_1(\mu x_6 + x_{05}, \mu y_6) p_2(x_6 - x_{05}, y_6) t(\mu x_6, \mu y_6) \times \exp \left[\frac{ik\mu^2}{2R} (x_6^2 + y_6^2) \right] \otimes P_0(x_6, y_6) \right|^2. \quad (56)$$

According to Eq. (56) within the overlap of the functions $p_1(\mu x_6 + x_{05}, \mu y_6)$, $p_2(x_6 - x_{05}, y_6)$, limiting the scatterer image formed in the hologram plane (Fig. 10b for $x_{05} = 3.5$ mm, $R = -330$ mm), the

subjective speckle structure is modulated by fringes of equal slope — a system of concentric rings. As the center of the filtering aperture displaces along the x axis, the behavior of the fringes is similar to that taking place in the case of formation of the scatterer image at the hologram recording shown in Fig. 1. In addition, the parallax of interference fringes is absent in both cases, as follows from the form of Eqs. (20) and (56) and from Fig. 10b.

Thus, the experimental investigations performed and the theoretical analysis of formation of interference patterns characterizing the transversal or longitudinal displacement of a diffusely scattering plane surface at double-exposure recording of the hologram of a focused image with the aid of a telecentric optical system have shown the following.

At the stage of reconstruction, interference patterns characterizing the transversal or longitudinal displacement of the scatterer are located in the hologram and in the Fourier plane. For the interference pattern located in the hologram plane, the interferometer sensitivity depends on the curvature radius of the spherical wave of the coherent radiation used to illuminate the scatterer and does not depend on the sign of the curvature radius. For the interference pattern located in the Fourier plane, the interferometer sensitivity depends on the focal length of the objective of the telecentric optical system. The parallax of interference fringes is absent, if the spatial filtering of the diffraction field is performed in the proper planes at the recording of interference patterns characterizing the longitudinal displacement of the scatterer. In addition, if the diffusely scattering plane surface is illuminated by the collimated beam at the stage of hologram recording, then the “frozen” interference pattern characterizing the transversal (or longitudinal) displacement of the scatterer is located in the Fourier plane. To record this pattern, it is not necessary to perform the spatial filtering of the diffraction field in the hologram plane.

References

1. V.G. Gusev, *Atmos. Oceanic Opt.* **19**, No. 1, 76–85 (2006).
2. V.G. Gusev, *Izv. Vyssh. Uchebn. Zaved. Fiz.* (2007) (in press).
3. J.W. Goodman, *Introduction to Fourier Optics* (McGraw–Hill, 1968).
4. V.G. Gusev, *Opt. i Spektrosk.* **69**, No. 5, 1125–1128 (1990).
5. V.G. Gusev, *Atmos. Oceanic Opt.* **6**, No. 9, 605–609 (1993).
6. M. Born and E. Wolf, *Principles of Optics* (Pergamon, New York, 1959).
7. R. Jones and C. Wykes, *Holographic and Speckle Interferometry* (Cambridge University Press, 1989).
8. V.G. Gusev, *Opt. i Spektrosk.* **74**, No. 5, 989–994 (1993).
9. V.G. Gusev, *Atmos. Oceanic Opt.* **10**, No. 7, 467–473 (1997).
10. L.M. Soroko, *Principles of Holography and Coherent Optics* (Nauka, Moscow, 1971), 601 pp.